COVER SHEET

NOTE:

- ***Please attach the signed copyright release form at the end of your paper and upload as a single 'pdf' file***
- ***This coversheet is intended for you to list your article title and author(s) name only***
- ***This page will not appear in the book or on the CD-ROM***

Title: *Simultaneous Strain and Temperature Sensing Using a Microstrip Patch Antenna for* Proceedings of the **11th International Workshop on Structural Health Monitoring 2017**

Authors: Franck Mbanya Tchafa
Haiying Huang

IMPORTANT All authors' information will appear on the program according to the submission stub on the online submission system (not to the manuscript). The title and author list provided in the manuscript will be for future referencing and citation.

PAPER DEADLINE: ****May 15, 2017****

PAPER LENGTH: ****8 PAGES MAXIMUM ****

Please submit your paper in PDF format. We encourage you to read attached Guidelines prior to preparing your paper—this will ensure your paper is consistent with the format of the articles in the CD-ROM.

NOTE: Sample guidelines are shown with the correct margins. Follow the style from these guidelines for your page format.

Hardcopy submission: Pages can be output on a high-grade white bond paper with adherence to the specified margins (8.5 x 11 inch paper). Please number your pages in light pencil or non-photo blue pencil at the bottom.

Electronic file submission: When making your final PDF for submission make sure the box at "Printed Optimized PDF" is checked. Also—in Distiller—make certain all fonts are embedded in the document before making the final PDF.

(FIRST PAGE OF ARTICLE)

ABSTRACT

In this paper, we present simultaneous strain and temperature sensing using a single microstrip patch antenna fabricated on commercial printed circuit board (PCB). Temperature and strain ~~are extracted~~ from the resonant frequencies of the patch antenna as these frequencies are dependent on the dielectric constant of the PCB and the patch dimensions, which are subject to change with applied strain and temperature variations. The principle of operation of the patch antenna is first discussed, followed by the design and fabrication of the instrumented test specimen. Finally, thermal and mechanical tests were conducted to validate the strain and temperature sensing performance of the antenna sensor.

INTRODUCTION

Patch antennas have been studied not only for wireless communication, but for structural health monitoring (SHM). Since the resonant frequency of a patch antenna depends on its dimensions and the dielectric constant of the substrate, any change in these parameters will cause a shift in the resonant frequency of the antenna. Therefore, one can use patch antennas as sensing elements by measuring changes in the patch dimensions and the dielectric constant of the PCB. In the past, patch antennas have been used for single-modality sensing of temperature, strain, crack, etc. [1] - [4]. They are convenient for SHM applications due to their low profile, ease of fabrication, low production cost, simple configuration, lightweight, and conformability to surfaces [5].

Wireless sensing using microstrip patch antennas is becoming increasingly popular as it eliminates the high maintenance cost usually associated with cable connections, especially for high temperature applications [5], [6]. Wireless sensors can be grouped into two categories: chip-based and chipless wireless sensors. In general, the main limitation of chip-based wireless sensors is the need for a battery on board to provide power to the microcontroller [7], [8]. As such, they are not suitable for harsh temperature SHM applications due to the limitation of the electronics on board. Moreover, their lifespan is limited by the battery life on board. In harsh temperature SHM applications, passive wireless sensors are the only feasible solution. Several passive wireless sensors have been proposed for SHM applications. Reindl and Shrena [9] proposed wireless

Surface Acoustic Wave (SAW) sensors for temperature sensing. However, it is difficult to miniaturize SAW sensors due to their low operation frequency. Also, SAW sensors can have high insertion loss, which limits their interrogation distance [10]. Wireless temperature sensing based on the antenna backscattering was demonstrated while achieving an interrogation distance of a few meters [11] - [13]. Due to mismatch of impedance between the antenna and the resistive load, the amplitude of the antenna backscattering will vary with temperature. Other wireless interrogation techniques for the antenna sensor were proposed. These techniques are: RFID-enabled techniques [14],[15], normalized Time Domain Reflectometry (TDR) [16], amplitude modulation and Frequency Modulated Continuous Wave (FMCW) interrogation [17]. The general limitation of these wireless interrogation techniques is that they require electronics at the sensor node. For high temperature SHM applications, Yao et al. in [1] demonstrated far-field interrogation of an antenna sensor without electronics by using a patch antenna as sensing element and a UWB antenna with a Reactive Impedance Surface (RIS) ground plane for wireless transmission [18]. The temperature information was encoded in the backscattered signals of the sensor node, and a TD gating technique was developed to extract the resonant frequency of the antenna sensor from the backscattered signal.

In this paper, we investigate multi-modality sensing of temperature and mechanical strain using a single microstrip patch antenna sensor fabricated on commercial substrate. Since we have previously demonstrated wireless interrogation of a high temperature antenna sensor without electronics [1], the anticipated outcome of this study is a wireless strain and temperature sensor that is easy to manufacture, and can be wirelessly interrogated from a long distance without electronics.

PRINCIPLE OF OPERATION

For this study, a rectangle was selected as the geometry of the microstrip patch antenna (RMPA). The RMPA consists of two conductive layers between which there is a dielectric substrate. Figure 1 illustrates a typical RMPA example. A RMPA does resonate at two precise fundamental frequencies that are distinguishable by the direction of the current flow. When current flows along the length and width directions of the RMPA, we have the TM_{010} and TM_{001} modes respectively. Per the transmission line model, the TM_{010} mode resonant frequency, f_{10}, can be calculated as

$$f_{10} = \frac{c}{2(L + 2\Delta L)\sqrt{\varepsilon_{re}}} \tag{1}$$

where c, L, ΔL, and ε_{re} represent the speed of light, the length of the patch antenna s, the line extension due to fringing, and the effective dielectric constant respectively [19]. The effective dielectric constant of the antenna ε_{re} and the line extension ΔL can

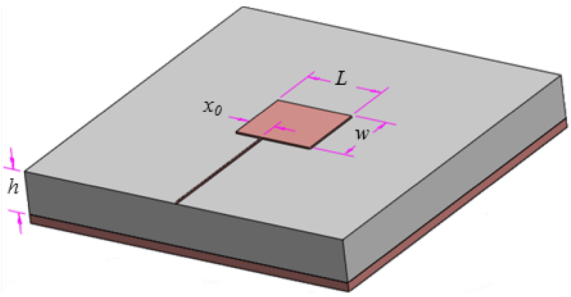

Figure 1. An illustration of a rectangular microstrip patch antenna

be expressed as

$$\varepsilon_{re} = \frac{\varepsilon_r + 1}{2} + \frac{\varepsilon_r - 1}{2\sqrt{1 + 10h/W}} \tag{2}$$

$$\Delta L = 0.412h \frac{(\varepsilon_{re} + 0.3)(W/h + 0.264)}{(\varepsilon_{re} - 0.258)(W/h + 0.813)} \tag{3}$$

The effective dielectric constant can be reduced to the dielectric constant of the substrate, and the line extension ΔL can be ignored if the height of the substrate is significantly smaller than the radiation patch dimensions (i.e. the patch antenna length and width). Given these assumptions, equation (1) can be simplified as

$$f_{10} = \frac{c}{2L\sqrt{\varepsilon_r}} \tag{4}$$

Expressing the patch antenna frequency shift δf_{10} in terms of changes in the patch length L and the substrate dielectric constant ε_r gives

$$\delta f_{10} = \frac{\partial f_{10}}{\partial \varepsilon_r}\delta\varepsilon_r + \frac{\partial f_{10}}{\partial L}\delta L \tag{5}$$

$\partial f_{10}/\partial \varepsilon_r$ and $\partial f_{10}/\partial L$ can be derived from (4), and the normalized resonant frequency shift $\delta f_{10}/f_{10}$ can be expressed as

$$\frac{\delta f_{10}}{f_{10}} = -\frac{1}{2}\frac{\delta\varepsilon_r}{\varepsilon_r} - \frac{\delta L}{L} \tag{6}$$

Both the patch antenna dimensions and the dielectric constant of the substrate are affected by temperature. In addition, the dimensions of the RMPA will change when strain is applied on the antenna sensor. Therefore, equation (6) can be further expanded into two parts to separate the contribution due to temperature and the contribution due to applied mechanical strain. Equation (6) can be rewritten as

$$\frac{\delta f_{10}}{f_{10}} = -\left(\frac{1}{2}\alpha_\varepsilon + \alpha_T\right)\delta T - \varepsilon_L \tag{7}$$

where ε_L is the applied strain along the patch length, α_T is the coefficient of thermal expansion of the substrate, α_ε is the thermal coefficient of dielectric constant (TCD_k) of the substrate [20]. Following the same approach, one can easily derive the normalized frequency shift of the TM_{001} mode. Assuming uniaxial loading conditions, a general equation of the normalized resonant frequencies for the TM_{010} and TM_{001} can be written as

$$\frac{\delta f_{10}}{f_{10}} = -K_{TL}\delta T - K_L\varepsilon_L \tag{8a}$$

and

$$\frac{\delta f_{01}}{f_{01}} = -K_{TW}\delta T + \nu K_W\varepsilon_L \tag{8b}$$

where v represents the Poisson's ratio, K_L and K_W represent the strain sensitivities along the patch length and width, and K_{TL} and K_{TW} represent the overall temperature sensitivities along the patch length and width respectively.

ANTENNA SENSOR DESIGN AND FABRICATION

Substrate Selection and Sensor Design

Based on equation (8) derived above, the substrate must be carefully selected to avoid the temperature sensitivity from overwhelming the strain sensitivity. For this study, we selected Rogers RT/duroid 5880 PCB given its material properties. The selected PCB has a dielectric constant ε_r of 2.2, a TCD_k of -125 ppm/^{o}C, and CTE values of 31 ppm/^{o}C, 48 ppm/^{o}C, and 237 ppm/^{o}C in x-, y-, and z- direction respectively. The sensor was designed to operate at 5 GHz and 6 GHz in the TM_{010} and TM_{001} modes respectively. Given the desired resonant frequencies of operation, the substrate thickness was selected as 0.79 mm to satisfy the requirement that the patch dimensions must be significantly greater than the substrate height. The antenna sensor is approximately 20 mm long and 16 mm wide. This gives an approximate width to height ratio of 20 and an approximate length to height ratio of 25. The radiating patch was fed by a transmission line that was matched to the TM_{010} mode and positioned at a distance x_o of 3.8 mm from the edge (see Figure 1).

Instrumented Test Specimen Design and Fabrication

To apply mechanical load on the antenna sensor, we designed a dog-bone specimen (DBS) on which the sensor will be bonded. The DBS was designed per the ASTM standards E8-04 and has a thickness of 2.3 mm and a gauge width of 40 mm. To determine a suitable gauge length that ensures uniaxial strain condition at the gauge area, the DBS was simulated using a finite element simulation tool ANSYS. First, a DBS with a gauge length of 60 mm was simulated and its stress distributions are shown

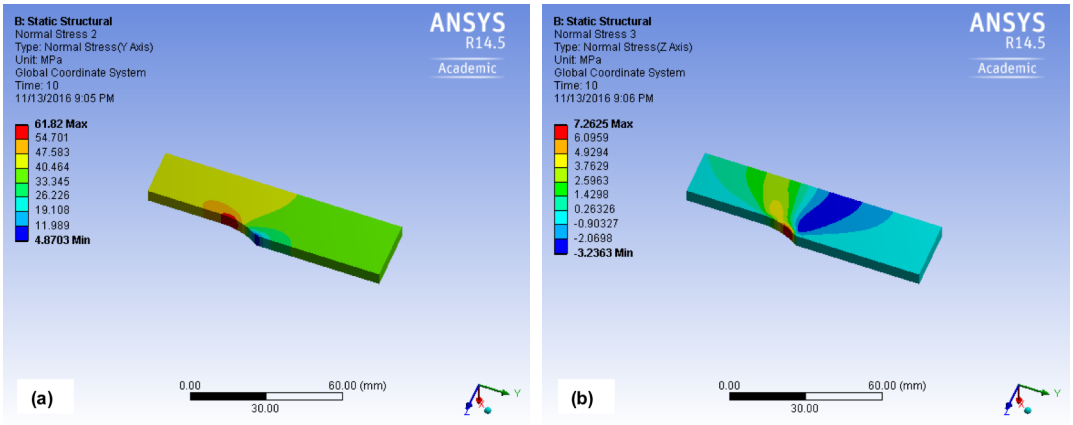

Figure 2. Simulated stress distribution on an aluminum dog bone with a gauge length and width of 60 mm and 40 mm respectively; (a) stress along the loading direction; (b) transverse stress.

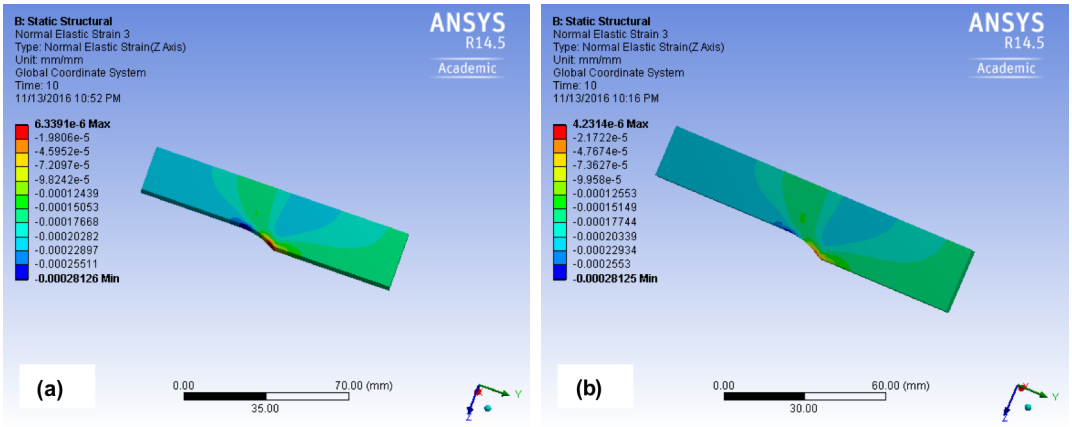

Figure 3. The effect of gauge length on the simulated stress distribution of an aluminum dog bone; (a) 85 mm; (b) 100 mm.

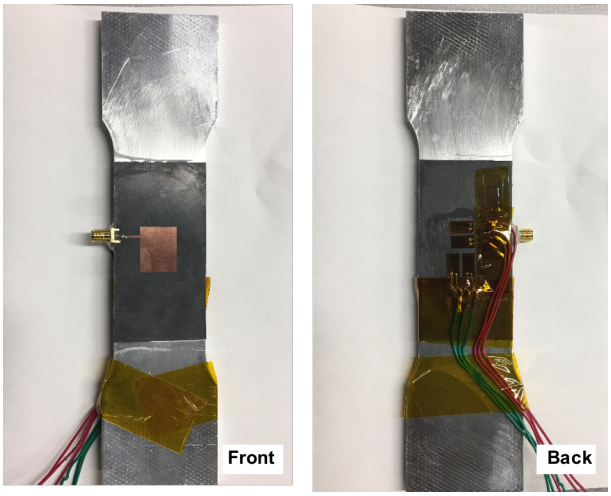

Figure 4. Aluminum 6061 dog-bone sample with the antenna sensor; (a) front view; (b) back view.

in Figure 2. Taking advantage of the symmetry of the DBS, only a quarter of the DBS was simulated. While the stress distribution along the loading direction is uniform at the center of the DBS (see Figure 2(a)), there seems to be stresses along the transverse direction and this stress distribution is not uniform, as shown in Figure 2(b). Clearly, the curvature at the transition between the gauge area and the gripping area generates transverse stress in the gauge area. Subsequently, a parametric study on various gauge lengths was carried out by keeping the gauge width at 40 mm and increasing the gauge length to 85 and then 100 mm. As shown in Figure 3, the transverse stress reduced substantially as the gauge length was increased to 85 mm. Further increase of the gauge length did not change the magnitude of the transverse stress; but the stress distribution is more uniform at the gauge area. Given the limitation of the tensile tester, we chose a gauge length of 85 mm for the DBS design. The new design was fabricated from an aluminum alloy 6061-T6. After fabricating the antenna sensor using chemical etching, the antenna sensor was bonded on the dog-bone sample using LOCTITE superglue. To ensure the symmetric configuration of the instrumented specimen, the same substrate used for fabricating the antenna sensor was also bonded on the back of the DBS. The

front and back views of the instrumented specimen are shown in Figure 4. OMEGA SGD5/350 LY13 strain gauges were bonded on the substrate in the back to measure the strains in both transverse and loading directions, as shown in Figure 4(b).

EXPERIMENTAL SETUP AND RESULTS

Mechanical Testing of the Instrumented Test Specimen

A QTest 150 tensile tester was used for mechanical testing of the new DBS and the experimental setup is shown in Figure 5. A personal computer running LabVIEW was used to acquire measurement data from the NI 9237 strain gauge module. The S-parameters of the antenna sensor were acquired using a Rhode & Schwarz ZVA24 Vector Network Analyzer (VNA) with a resolution set at 75 kHz. Tensile loads were applied on the DBS in increments of 450 lbf (1000 N). At each load, the DBS was let to rest for 43 seconds before taking any measurements. 5 readings were taken at each applied load and the results are presented in Figure 6. The antenna sensor displayed a strain sensitivity of 0.79 ppm/microstrain along the loading direction and a transverse strain sensitivity of 0.29 ppm/microstrain. The ratio between the transverse and longitudinal strain sensitivities is 0.36, which is in good agreement with the Poisson's ratio of 0.33 for Aluminum 6061-T6. These results validate that the selected dog-bone gauge length is suitable for future thermo-mechanical testing as it ensures uniaxial loading on the antenna sensor. The antenna frequency along the transverse direction displays some fluctuations, as shown in Figure 6. We believe that these fluctuations are due to the lack of annealing for the adhesive material. Despite the fluctuations, the R-square values for the antenna frequencies along the loading and transverse directions are 0.9865 and 0.9595, respectively, indicating both antenna frequencies varied linearly with the applied strain.

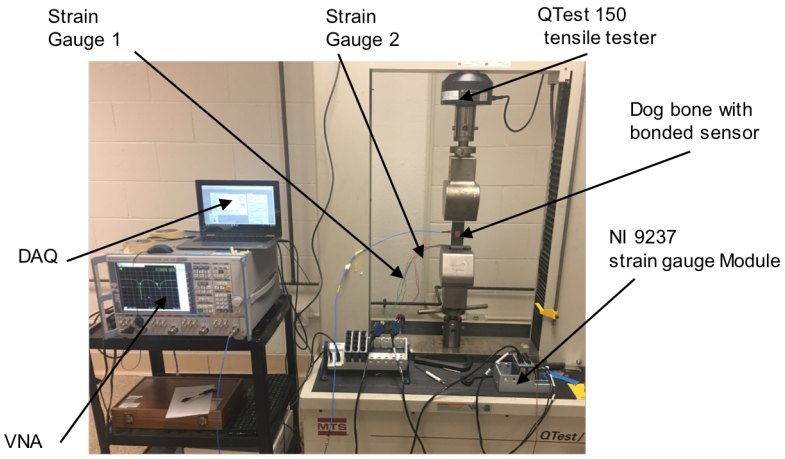

Figure 5. Experimental set up for mechanical testing of the antenna sensor

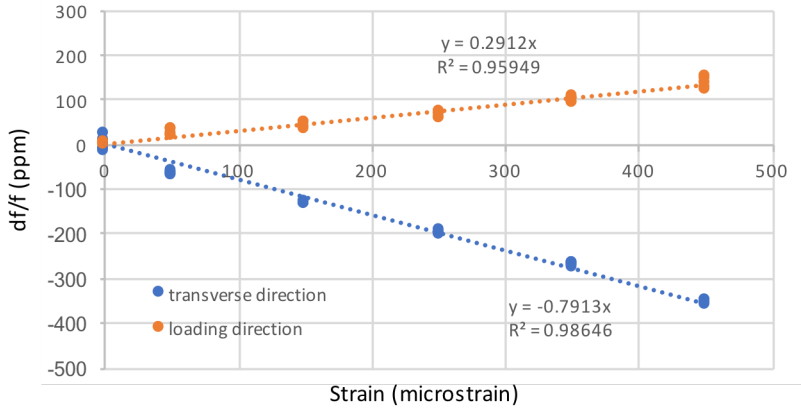

Figure 6. Measured relationship between the antenna resonant frequencies and the applied strain. The ratio between the strain sensitivity in both directions agrees with the theoretical prediction.

Thermal Testing of the Instrumented Test Specimen

After validating the antenna sensor's performance for strain measurements, thermal tests of the DBS were conducted inside a high temperature furnace from Thermo Fisher, as shown in Figure 7. The S-parameters of the antenna sensor were acquired using the R&S ZVA24 VNA, and temperature was measured using an OMEGA T-type thermocouple. The experiment was controlled using a personal computer running LabVIEW. Each temperature and sensor scattering parameters reading were time stamped for ease of data analysis, and to minimize the time difference between the temperature and sensor reading. The sample was first subjected to a few cycles of heating and cooling before measurements. The sensor was heated up at a slow rate of 2°C per minute. At each temperature reading, 4 sensor's measurements were acquired. Figure 8 shows the experimental results obtained from the sensor. The data display good linearity with a sensitivity of 30 ppm/°C for the TM_{010} mode and 26 ppm/°C for the TM_{001} mode. The expected sensitivity is 39.1 ppm/°C given the manufacturer's specified TCDk value of -125 ppm/°C, and 23.4 ppm/°C for the coefficient of thermal expansion of the Aluminum 6061-T6. As per the manufacturer, the TCDk needs to be calibrated based on experiment. Based on the experimental results, we can derive the

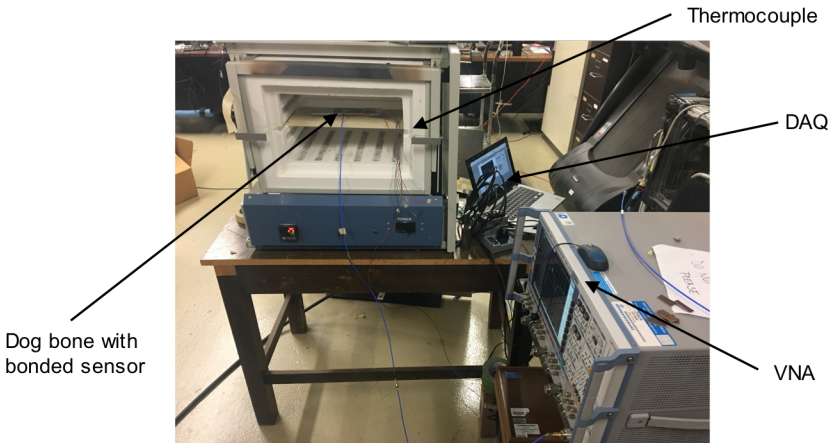

Figure 7. Experimental set up for thermal testing of the antenna sensor.

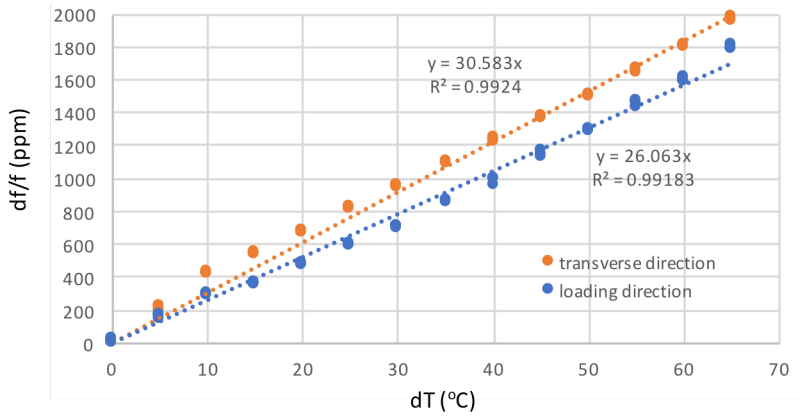

Figure 8. Measured temperature sensitivity of the antenna sensor.

average TCDk to be -106.3 ppm/°C. These results demonstrate that the TCDk of the substrate material is sensitive to temperature variations yet is not too large to overwhelm the strain sensitivity of the antenna sensor.

CONCLUSION

In this paper, we have demonstrated temperature and strain sensing of the proposed sensor by subjecting the fabricated antenna sensor to thermal and mechanical tests. Given the results presented, we are confident that the proposed sensor will perform well while being subjected to simultaneous strain and temperature testing. Also, since we have demonstrated wireless capability of the antenna sensor in the past, the anticipated outcome of this research is a wireless temperature and strain sensor that can be interrogated from a long distance without electronics at the sensor nodes. This research will likely impact the design of future patch antenna sensor for harsh environment SHM applications. In the future, the present sensor will be subjected to thermo-mechanical tests. In addition, the wireless capability of the sensor will be demonstrated. Finally, a high-temperature PCB material will be developed to achieve higher temperature wireless sensing capability.

ACKNOWLEDGMENTS

This material is based upon work supported by the Department of Energy under Award Number DE-FE0023118. This report was prepared as an account of work sponsored by an agency of the United States Government. Neither the United States Government nor any agency thereof, nor any of their employees, makes any warranty, express or implied, or assumes any legal liability or responsibility for the accuracy, completeness, or usefulness of any information, apparatus, product, or process disclosed, or represents that its use would not infringe privately owned rights. Reference herein to any specific commercial product, process, or service by trade name, trademark, manufacturer, or otherwise does not necessarily constitute or imply its endorsement, recommendation, or favoring by the United States Government or any agency thereof. The views and opinions of authors expressed herein do not necessarily state or reflect those of the United States Government or any agency

thereof.

REFERENCES

1. J. Yao *et al*. Far-field interrogation of microstrip patch antenna for temperature sensing without electronics. *IEEE Sensors Journal 16(19),* pp. 7053-7060. 2016. DOI: 10.1109/JSEN.2016.2597739.
2. U. Tata, H. Huang, R. L. Carter, and J. C. Chiao, "Exploiting a patch antenna for strain measurements," *Meas. Sci. Technol.*, vol. 20, p. 015201, 2008.
3. J. Sanders, J. Yao, and H. Huang, "Microstrip Patch Antenna Temperature Sensor," *IEEE Sens. J.*, vol. 15, no. c, pp. 1–1, 2015.
4. X. Xu and H. Huang, "Multiplexing passive wireless antenna sensors for multi-site crack detection and monitoring," *Smart Mater. Struct.*, vol. 21, p. 015004, 2011.
5. H. Huang, "Flexible wireless antenna sensor: A review," *IEEE Sensors Journal*, vol. 13, no. 10. pp. 3865–3872, 2013.
6. A. Deivasigamani, A. Daliri, C. H. Wang, and S. John, "A review of passive wireless sensors for structural health monitoring," *Modern Applied Science*, vol. 7, no. 2. pp. 57–76, 2013.
7. I. F. Akyildiz, W. Su, Y. Sankarasubramaniam, and E. Cayirci, "A survey on sensor networks," *IEEE Commun. Mag.*, vol. 40, no. 8, pp. 102–105, 2002.
8. J. Yick, B. Mukherjee, and D. Ghosal, "Wireless sensor network survey," *Comput. Networks*, vol. 52, no. 12, pp. 2292–2330, 2008.
9. L. M. Reindl and I. M. Shrena, "Wireless measurement of temperature using surface acoustic waves sensors," *IEEE Trans. Ultrason. Ferroelectr. Freq. Control*, vol. 51, no. 11, pp. 1457–1463, 2004.
10. A. Pohl, "A review of wireless SAW sensors.," *IEEE Trans. Ultrason. Ferroelectr. Freq. Control*, vol. 47, no. 2, pp. 317–332, 2000.
11. S. Bouaziz, F. Chebila, A. Traille, P. Pons, H. Aubert, and M. M. Tentzeris, "Novel microfluidic structures for wireless passive temperature telemetry medical systems using radar interrogation techniques in ka-band," *IEEE Antennas Wirel. Propag. Lett.*, vol. 11, pp. 1706–1709, 2012.
12. D. Girbau, Á. Ramos, A. Lazaro, S. Rima, and R. Villarino, "Passive wireless temperature sensor based on time-coded UWB chipless RFID tags," *IEEE Trans. Microw. Theory Tech.*, vol. 60, no. 11, pp. 3623–3632, 2012.
13. K. Opasjumruskit *et al.*, "Self-powered wireless temperature sensors exploit RFID technology," *IEEE Pervasive Computing*, vol. 5, no. 1. pp. 54–61, 2006.
14. X. Yi, T. Wu, Y. Wang, R. T. Leon, M. M. Tentzeris, and G. Lantz, "Passive wireless smart-skin sensor using RFID-based folded patch antennas," *Int. J. Smart Nano Mater.*, vol. 2, pp. 22–38, 2011.
15. Q. Qiao, L. Zhang, F. Yang, Z. Yue, and A. Z. Elsherbeni, "Reconfigurable sensing antenna with novel HDPE-BST material for temperature monitoring," *IEEE Antennas Wirel. Propag. Lett.*, vol. 12, pp. 1420–1423, 2013.
16. S. Deshmukh and H. Huang, "Wireless interrogation of passive antenna sensors," *Meas. Sci. Technol.*, vol. 21, no. 3, p. 35201, 2010.
17. J. Yao, S. Tjuatja, and H. Huang, "Real-Time Vibratory Strain Sensing Using Passive Wireless Antenna Sensor," *IEEE Sens. J.*, vol. 15, no. 8, pp. 4338–4345, 2015.
18. H. Mosallaei and K. Sarabandi, "Antenna Miniaturization and Bandwidth Enhancement Using a Reactive," *IEEE Trans. Antennas Propag.*, vol. 52, no. 9, pp. 2403–2414, 2004.
19. C. E. Balanis, "Antenna Theory: Analysis and Design, 3rd Edition - Constantine A. Balanis," *Book*. p. 1136, 2005.
20. K. R. Carver and J. W. Mink, "Microstrip Antenna Technology," *IEEE Trans. Antennas Propag.*, vol. 29, no. 1, pp. 2–24, 1981.

DEStech Publications, Inc.

CONTRIBUTING AUTHOR COPYRIGHT RELEASE FORM

As author of the chapter/contribution titled _____
_____, to appear in the *Proceedings of Structural Health Monitoring 2017*, I hereby agree to the following:

1. To grant to DEStech Publications, Inc., 439 North Duke Street, Lancaster, PA, 17602, copyright of the above named chapter/contribution (for U.S. Government employees to the extent transferable), in print, electronic, and online formats. However, the undersigned reserve the following:
a. All proprietary rights other than copyright, such as patent rights.
b. The right to use all or part of this article in future works.

DEStech Publications thereby retains full and exclusive right to publish, market, and sell this material in any and all editions, in the English language or otherwise.

1 I warrant to DEStech Publications, Inc., that I am the (an) author of the above-named chapter/contribution and that I am the (a) copyright holder of the above-named chapter/contribution granted to DEStech Publications, Inc.

2 I warrant that, where necessary and required, I have obtained written permission for the use of any and all copyrighted materials used in the above-named chapter/contribution. I understand that I am responsible for all costs of gaining written permission for use of copyrighted materials.

3 I agree to assume full liability to DEStech Publications, Inc. and its licensee, and to hold DEStech Publications, Inc. harmless for any claim or suit filed against DEStech Publications, Inc. for violation of copyrighted material used in the above-named contribution.

Please sign and date this form and retain a copy for your records. Please include original form with your chapter/paper.

Thank you for your cooperation.

Please print name: _____
Signed: _____Dated: _____

439 NORTH DUKE STREET • LANCASTER, PENNSYLVANIA 17602-4967, U.S.A. Toll Free: (866) 401-4337 • Tel: (717) 290-1660 • Fax: (717) 509-6100 E-mail: info@destechpub.com • Internet address: www.destechpub.com